



Macrophage contribution to the survival of transferred expanded skin flap through angiogenesis

Zhaosong Huang^{#^}, Jianke Ding^{#^}, Yajuan Song[^], Wei Liu[^], Chen Dong[^], Yu Zhang[^], Tong Wang, Jing Du[^], Shaoheng Xiong[^], Qiang He[^], Zhou Yu[^], Xianjie Ma[^]

Department of Plastic Surgery, Xijing Hospital, Fourth Military Medical University, Xi'an, China

Contributions: (I) Conception and design: X Ma, Z Yu, J Ding; (II) Administrative support: T Wang, Q He; (III) Provision of study materials or patients: Z Huang, W Liu, C Dong, Y Zhang, J Du; (IV) Collection and assembly of data: Z Huang, S Xiong, Y Song, W Liu; (V) Data analysis and interpretation: Z Huang, J Ding, C Dong, Y Zhang, Z Yu; (VI) Manuscript writing: All authors; (VII) Final approval of manuscript: All authors.

[#]These authors contributed equally to this work and should be considered as co-first authors.

Correspondence to: Zhou Yu, MD, PhD; Xianjie Ma, MD, PhD. Department of Plastic Surgery, Xijing Hospital, Fourth Military Medical University, Xi'an 710032, China. Email: yz20080512@163.com; majing@fmmu.edu.cn.

Background: Despite the application of tissue expansion in the reconstruction of significant tissue defects, complications with expanded random-pattern skin flaps remain a major challenge. Insufficient angiogenesis is one of the keys factors in flap ischemia and dysfunction. Macrophages play a key role in promoting tissue angiogenesis, but their effects on expanded flap angiogenesis and the survival of the transferred skin flap are still unknown.

Methods: A rat scalp expansion model was established to evaluate the dynamic changes of macrophages in expanded skin. Clodronate liposomes (Clo-lipo) were injected into the expanded scalps to deplete the macrophages, and the expanded scalp flaps with macrophage depletion were orthotopically transferred. The remaining expanded rat scalp flaps were treated with either a macrophage-colony stimulating factor (M-CSF) alone or M-CSF in combination with Clo-lipo and transferred. The number of macrophages, blood perfusion, microvascular densities (MVDs), flap survival, histological changes, and gene expression related to macrophage polarization and angiogenesis were determined with immunofluorescence (IF) staining, full-field laser perfusion imager, hematoxylin and eosin (HE) staining, and quantitative real-time polymerase chain reaction.

Results: The number of pan-macrophages significantly increased in the expanded scalp on days 14 and 21 after expander placement. The depletion rate after treatment with Clo-lipo was 29.06%, and the number of macrophages was significantly reduced in the group that underwent Clo-lipo treatment on day 14 before flap transfer ($P < 0.05$). Macrophage depletion resulted in decreased blood perfusion, reduced MVDs, lower expression of factors, and poor survival rate. The recruitment of macrophages with a M-CSF led to higher blood perfusion, increased MVDs, greater expression of angiogenic factors, and better flap survival after flap transfer.

Conclusions: Alternatively activated macrophages in the expanded flap could significantly promote angiogenesis, improve blood perfusion, and ultimately increase the flap survival rate. Modulating alternatively activated macrophages may provide a key therapeutic strategy to promote expanded skin flap survival. Our study has provided a basis for clinically improving random-pattern skin flap survival.

[^] ORCID: Zhaosong Huang, 0000-0002-6151-4967; Jianke Ding, 0000-0001-9440-2489; Yajuan Song, 0000-0002-5700-9909; Wei Liu, 0000-0001-6739-9990; Chen Dong, 0000-0002-1189-5458; Yu Zhang, 0000-0001-9463-4263; Jing Du, 0000-0001-7446-202X; Shaoheng Xiong, 0000-0002-5550-0518; Qiang He, 0000-0002-4714-4533; Zhou Yu, 0000-0002-2358-0090; Xianjie Ma, 0000-0001-5462-0895.

Keywords: Tissue expansion; random-pattern flap; macrophages; angiogenesis; survival

Submitted Mar 23, 2022. Accepted for publication Oct 30, 2022. Published online Jan 30, 2023.

doi: 10.21037/atm-22-1558

View this article at: <https://dx.doi.org/10.21037/atm-22-1558>

Introduction

Skin expansion can harvest “extra skin tissue” that is similar in texture, color, and flexibility to the adjacent tissues. Random-pattern expanded skin flaps refer to expanded skin flaps with nonspecific blood circulation and are routinely used to reconstruct defects from injuries, ulcerations, tumor excision, and malformation (1). The length-to-width ratio is normally restricted to 1.5 or 2, but it can be widened to 3 in facial-neck regions with sufficient blood supply (2). As random-pattern flaps are formed without retaining the vascular pedicle, partial or complete necrosis remains a serious complication in random-pattern expanded skin flap transfers (3). Additionally, subcutaneous hematoma or infection in flap tissue is generally considered a result of insufficient blood supply and inadequate angiogenesis (4).

A recent study indicates a strong connection between inflammatory and regenerative processes. Macrophages play a key role in coordinating these processes and are essential for recovering tissue integrity and function (5). Angiogenesis is a complex process involving proliferation, migration, and differentiation of vascular endothelial cells (ECs) under

the stimulation of specific signals. It is controlled by the balance between promoting and inhibiting factors. Various angiogenic factors produced by macrophages have been identified that function in stimulating angiogenesis (6). Angiogenesis and vascular remodeling and maturation are essential for tissue regeneration. The inhibition of macrophage activity reduces angiogenesis, demonstrating the contribution of macrophages to the revascularization of regenerating tissue (7). Macrophages critically contribute to wound healing by angiogenic processes (8). The mechanisms that promote skin regeneration and skin flap survival are currently under investigation. Our previous research suggested that macrophages are necessary for skin regeneration during tissue expansion (9); however, the effects of macrophages on the angiogenesis of expanded flap and the survival of the transferred random-pattern skin flap remain unknown.

We hypothesized that macrophage depletion during expansion would reduce expanded random-pattern skin flap survival through the inhibition of angiogenesis. This hypothesis was tested by establishing both macrophage depletion and macrophage recruitment models and comparing the following outcomes: number of macrophages, blood perfusion, number of blood vessels, flap survival, histological changes, and gene expression related to macrophage polarization and angiogenesis. We present the following article in accordance with the ARRIVE reporting checklist (available at <https://atm.amegroups.com/article/view/10.21037/atm-22-1558/rc>).

Methods

Rat scalp expansion model

In total, 75 male Sprague Dawley rats (6 weeks old; 160–180 g) were purchased from the Experimental Animal Center of the Fourth Military Medical University. The rats were housed in separate cages (6 rats per cage) under a temperature of 23 °C, a relative humidity of 55%±5%, and a 12-hour light-dark cycle. The rats had free access to standard chow and water. To evaluate the histological

Highlight box

Key findings

- M2 macrophages in the expanded flap could significantly promote angiogenesis, improve blood perfusion, and ultimately increase the flap survival rate.
- Modulating M2 macrophages and relevant angiogenic factors may provide a key therapeutic strategy to promote the survival rate of expanded skin flap after transfer.

What is known and what is new?

- Macrophages play a key role in promoting tissue angiogenesis.
- Our study has provided a basis for clinically improving transferred random-pattern skin flap survival.

What is the implication, and what should change now?

- The specific macrophage subtypes that give rise to distinct roles in the angiogenesis and flap survival remained unexamined.
- Selective M1/M2 macrophage depletion should be done in further research.

changes and macrophage infiltration in the expanded scalp tissues, the rats were randomly divided into an expanded scalp group (n=18) and a sham group (n=18). The surgery for tissue expansion was described in our previous study (10). Briefly, a 1-milliliter silicone expander was placed under the scalp on the preperiosteal plane. The sham group underwent the same surgical process but received a silicone sheet without saline injection. Subsequently, 1 mL of sterilized saline was injected to flatten the silicone expander. Sterilized saline was injected every 2 days in the expanded group (0.7 mL per injection) until the silicone expander was enlarged to a volume of 5.9 mL on day 14. The time of expander implantation was designated on day 0. On days 7, 14, and 21 after expander implantation, expanded scalp tissues from 6 rats in each group at each time point were subjected to hematoxylin and eosin (HE) staining and immunofluorescence (IF) staining to determine the number of macrophages and histologic changes. Experiments were performed under a project license (No. IACUC-20181209) granted by the Experimental Animal Committee of the Fourth Military Medical University, and all animal surgeries were strictly performed in accordance with the institutional guidelines for the care and use of animals. A protocol was prepared before the study without registration.

Macrophage depletion in the rat scalp expansion model

The 23 rats that underwent scalp expansion were randomly divided into a clodronate liposome (Clo-lipo) group (n=12) and a phosphate-buffered saline liposome (PBS-lipo) group (n=11). To deplete the macrophages in the expanded flaps, 50 μ L of Clo-lipo (50 μ g/mL; Liposoma, Amsterdam, the Netherlands) was injected subcutaneously into the expanded scalps of rats in the Clo-lipo group on days 0, 4, 8, and 12 (9). The rats in the PBS-lipo group were subcutaneously injected with 50 μ L of PBS-lipo (50 μ g/mL; Liposoma) as a control. The scalp expansion surgery and saline injection were performed as in the rat scalp expansion model. Treatments were administered for 2 weeks, after which the expanded scalp tissues of 6 rats from each group were removed and analyzed with IF staining to test the depletion efficiency of macrophages in the expanded scalp skin. Meanwhile, the scalp flaps of the remaining rats (Clo-lipo group: n=6; PBS-lipo group: n=5) were orthotopically transferred on day 14 and excised 7 days after flap transfer (day 21) to investigate the effects of macrophage depletion on angiogenesis in the transferred scalp flap.

Macrophage-colony stimulating factor (M-CSF) treatment alone and combined with Clo-lipo

To further evaluate the effects of macrophage recruitment on angiogenesis in the transferred scalp flap, 16 rats were randomly divided into 3 groups: a PBS group (n=6), a M-CSF treatment group (n=5), and a combined M-CSF/Clo-lipo treatment group (n=5). Subsequently, 50 μ L of recombinant rat M-CSF protein (ab269198; Abcam, Cambridge, UK) at a 20 ng/ μ L concentration was injected into the expanded scalp of rats in the M-CSF group, while the combined M-CSF/Clo-lipo group received a combined injection of both M-CSF and Clo-lipo at the same volume. Injected M-CSF preferentially recruits macrophages to the expanded scalp, whereas Clo-lipo injection is used to deplete macrophages in the expanded scalp. The same volume of PBS was used as a control. For rats, M-CSF was injected subcutaneously on postoperative days 0, 2, 4, 6, 8, 10, 12, and 14 (11); and Clo-lipo was injected subcutaneously on postoperative days 0, 4, 8, and 12. The surgery and expansion process were performed as previously stated. Tissue biopsies were performed on day 21 after expander placement, and samples were subjected to HE and IF staining.

Expanded random-pattern flap transfer

Orthotopic transfer of the expanded random-pattern flap model was established using the rats which had undergone scalp expansion with macrophage depletion. The time of expander implantation was designated as day 0. All expanded random-pattern scalp flap transfers were performed on day 14 after expander placement. First, rats were anesthetized with isoflurane (5% induction and 2% maintenance), and the cephalic skin flap (1 cm \times 3 cm) was then outlined on the rat's expanded scalp. Then, both supraorbital arteries in the flap pedicle end were identified and ligated using a 9-0 polyester suture. After the expander was removed and excess skin was trimmed, the flap was immediately sutured to the orthotopic donor bed using 5-0 silk sutures. Finally, the scalp flap was packaged and bandaged under pressure, with the pressure increasing gradually from the caudal base to the distal flap. The survival of the scalp flaps was recorded 7 days after expanded flap transfer surgeries (day 21) using a digital camera at 30 cm from the area of the scalp flaps after the rats were positioned. The survived area of the skin flap was measured using ImageJ software 1.8.0 (National Institutes of Health, Bethesda, MD, USA). The expanded

random-pattern flap samples were obtained, after which the animals were killed (day 21). Flap blood flow perfusion imaging was obtained in anesthetized rats *in vivo* on day 21, after which flap tissues were excised and subjected to flap survival analysis, HE and IF staining, and quantitative real-time polymerase chain reaction (qRT-PCR).

Histologic examination

Skin samples were fixed in 10% formaldehyde solution for at least 24 hours, embedded in paraffin, sectioned at 5 μm , stained with HE, and examined microscopically according to routine procedures. Expanded scalp samples (n=6 per group at each time point) were procured on days 7, 14, and 21. If necrosis occurred, samples were taken from the remaining viable flap tissue.

Blood flow measurements

On day 21, the regional microvascular blood flow intensity of scalp flaps that had undergone random-pattern expanded flap transfer was continuously quantified in anesthetized rats *in vivo* using a full-field laser perfusion imager (FLPI; Moor FLPI, Moor Instruments Ltd., Devon, UK). The blood flow intensity was recorded as the flux perfusion unit (PU) and calculated using image processing software (Moor FLPI 3.0). Blood flow was calculated as the mean value of 10 independent images for each rat.

IF staining

For IF staining, tissue sections were rehydrated, submitted to an antigen retrieval step at 96 °C for 20 minutes in citrate buffer at a pH of 6.0, and blocked for 1 hour. Following this, primary antibody was applied to the tissue overnight at 4 °C in a humid chamber; tissue sections were then stained with conjugated secondary antibodies and finally counterstained with 4',6-diamidino-2-phenylindole. Primary antibodies against the pan-macrophage marker mouse anti-rat CD68 antibody (1:100; ab31630; Abcam), M1 macrophage marker rabbit anti-rat inducible nitric oxide synthase antibody (iNOS; 1:25; ab15323; Abcam), M2 macrophage marker CD206 antibody (1:50; ab64693; Abcam), and angiogenesis marker CD34 antibody (1:100, ab81289, Abcam) were used. To determine the number of pan-macrophages, samples of expanded and sham scalp groups were labeled with a CD68 antibody on days 7, 14, and 21. Expanded scalp sections of Clo-lipo and PBS-lipo treatment groups on days 14 were

screened with a CD68⁺ macrophage depletion efficiency. IF staining was used to label the M1 (iNOS⁺CD68⁺) and M2 (CD206⁺CD68⁺) macrophages on day 21. CD34⁺ was used to determine the number of blood vessels in transferred random-pattern expanded flaps. Slides were imaged at 25 °C at $\times 20/\times 40$ magnification using the Nikon A1 HD25 confocal microscope (Nikon Instruments Inc., Melville, NY, USA). Six random fields per section were captured and analyzed with NIS-Elements Viewer 4.20 software (Nikon Instruments Inc.).

Quantitative real-time polymerase chain reaction

The messenger RNA (mRNA) levels of CD68, colony-stimulating factor 1 receptor (CSF-1R), iNOS, platelet-derived growth factor receptor (PDGFR), fibroblast growth factor (FGF), vascular endothelial growth factor α (VEGF α), and C-X-C motif chemokine ligand 10 (CXCL10) were measured qRT-PCR. The total RNA was extracted from random-pattern expanded flap tissues after flap transfer on day 21 using TRIzol reagent (Invitrogen, Thermo Fisher Scientific, Waltham, MA, USA). Briefly, an 80 mg to 100 mg portion of the flap was homogenized in 1 mL of Trizol reagent. Postcentrifugation, RNA was extracted with chloroform and precipitated with isopropyl alcohol. Isolated RNA samples were then reverse-transcribed into complement DNA (cDNA) using a cDNA synthesis kit (Takara Bio Inc., Shiga, Japan) following standard protocols. Quantitative gene expression was detected using synthetic primers and SYBR Green (Takara Bio Inc.). Relative mRNA levels were normalized to GAPDH. The primers used are listed in Table S1.

Statistical analysis

All data in this study are expressed as the mean \pm standard error. Statistical analyses were performed using GraphPad Prism 8.0.2 (GraphPad Prism 8.0.2, GraphPad Software, San Diego, CA, USA). Statistical significance was determined using *t*-tests between 2 groups or 1-way analysis of variance (ANOVA) with Bonferroni correction for multiple comparisons.

Results

Dynamic changes of macrophage number in the expanded scalp

A rat scalp expansion model was established to evaluate

the dynamic changes of macrophages and the thickness of expanded skin (Figure 1A,1B). The thickness of the expanded scalp group was thinner than that of the sham group on days 14 and 21 ($P < 0.01$), although there was no significant difference on day 7 ($P > 0.05$; Figure 1C,1D). Similarly, the number of pan-macrophages was significantly higher in the expanded scalp group than in the sham group on days 14 ($P < 0.05$) and 21 ($P < 0.001$); however, there was no significant difference on day 7 ($P > 0.05$; Figure 1E,1F).

Macrophage depletion decreased the survival rate and thickness of expanded scalp flap after transfer

In the expanded scalp group, the number of CD68⁺ macrophages was significantly increased compared to the sham group on day 14. A model of macrophage depletion in the rat scalp expansion and expanded random-pattern flap transfer was established to evaluate the flap survival rate after macrophage depletion (Figure 2A). IF staining indicated that the number of macrophages was markedly reduced in the group that underwent Clo-lipo treatment on day 14 before flap transfer ($P < 0.05$; Figure 2B,2C), indicating the depletion of macrophages in the expanded scalp. No side effects (including death) were observed during the macrophage depletion prior to flap transfer; however, after flap transfer, the average flap survival area was smaller in the Clo-lipo group ($37.32\% \pm 10.66\%$) than in the PBS-lipo group ($51.73\% \pm 8.27\%$; $P < 0.05$; Figure 2D,2E) on day 21. In addition, the expanded flaps in the Clo-lipo group were thinner than those in the PBS-lipo group ($P < 0.05$; Figure 2F,2G).

The number of M2 macrophages reduced significantly in the Clo-lipo group after expanded scalp flap transfer

To understand how macrophages influence the survival of random-pattern expanded scalp flap, subtypes of macrophages were identified. In contrast to the PBS-lipo treatment group, the Clo-lipo group had a significantly decreased total number of macrophages ($P < 0.01$). Further study revealed that the number of M2 macrophages in the expanded scalp was decreased in the Clo-lipo group ($P < 0.01$), although there was no difference in the number of M1 macrophages between groups (Figure 3A-3D; $P > 0.05$). We further examined the expression of macrophage-related biomarkers with qRT-PCR (Figure 3E-3G). The mRNA expression of CD68 and CSF-1R was markedly downregulated (Figure 3E,3F, $P < 0.05$), while no significant

difference was found in iNOS mRNA expression after macrophage depletion (Figure 3G; $P > 0.05$). These results showed that the liposome clodronate injection mainly decreased the number of M2 macrophages, suggesting that these play an important role in expanded scalp flap survival in this model.

Macrophage depletion inhibited angiogenesis of the transferred expanded scalp flaps

To investigate the effects of macrophage depletion on angiogenesis in the transferred scalp flap, blood perfusion, microvascular densities (MVDs), and the expression of angiogenic factors were analyzed. The PBS-lipo group showed higher ($P < 0.05$; Figure 4A,4B) blood perfusion ($258.73 \pm 37.56/\text{flux}$) compared to the Clo-lipo group ($191.88 \pm 42.51/\text{flux}$). The number of CD34⁺ blood vessels was smaller in the Clo-lipo group ($15.65 \pm 6.01/\text{per field}$) than in the PBS-lipo group ($27.83 \pm 8.66/\text{per field}$; $P < 0.001$; Figure 4C,4D). The results of qRT-PCR in the depleted group showed decreased expression of PDGFR and FGF ($P < 0.05$; Figure 4E) but increased expression of the angiostatic factor CXCL10 ($P < 0.05$; Figure 4E). Surprisingly, no significant differences were detected in the expression of VEGF α between the 2 groups (Figure 4E).

Macrophage recruitment with M-CSF injection during expansion increased the transferred flap survival

To further understand the role of macrophages on the expanded scalp flap, another assay was performed to assess the survival and thickness of flaps. The expanded flaps were subcutaneously injected with PBS (PBS group: $n=6$), M-CSF (macrophage recruitment, M-CSF group: $n=5$), or M-CSF combined with Clo-lipo (M-CSF + Clo group: $n=5$) at distinct time points; the expanded scalp flaps were then orthotopically transferred (Figure 5A). Compared with that in M-CSF group, the survival areas of the transferred expanded flaps in the PBS group (1-way ANOVA, $P < 0.001$; Figure 5B,5C) and M-CSF + Clo group (1-way ANOVA, $P < 0.05$; Figure 5B,5C) were decreased. No significant difference was observed between the PBS and M-CSF + Clo groups (Figure 5B, 5C). A thicker epidermis (1-way ANOVA, $P < 0.001$; Figure 5D,5E) and dermis (1-way ANOVA, $P < 0.05$; Figure 5D,5E) were found in the M-CSF group, whereas this effect in the epidermis (1-way ANOVA, $P < 0.001$; Figure 5D,5E) and dermis (1-way ANOVA, $P < 0.01$; Figure 5D,5E) was reversed in the M-CSF + Clo

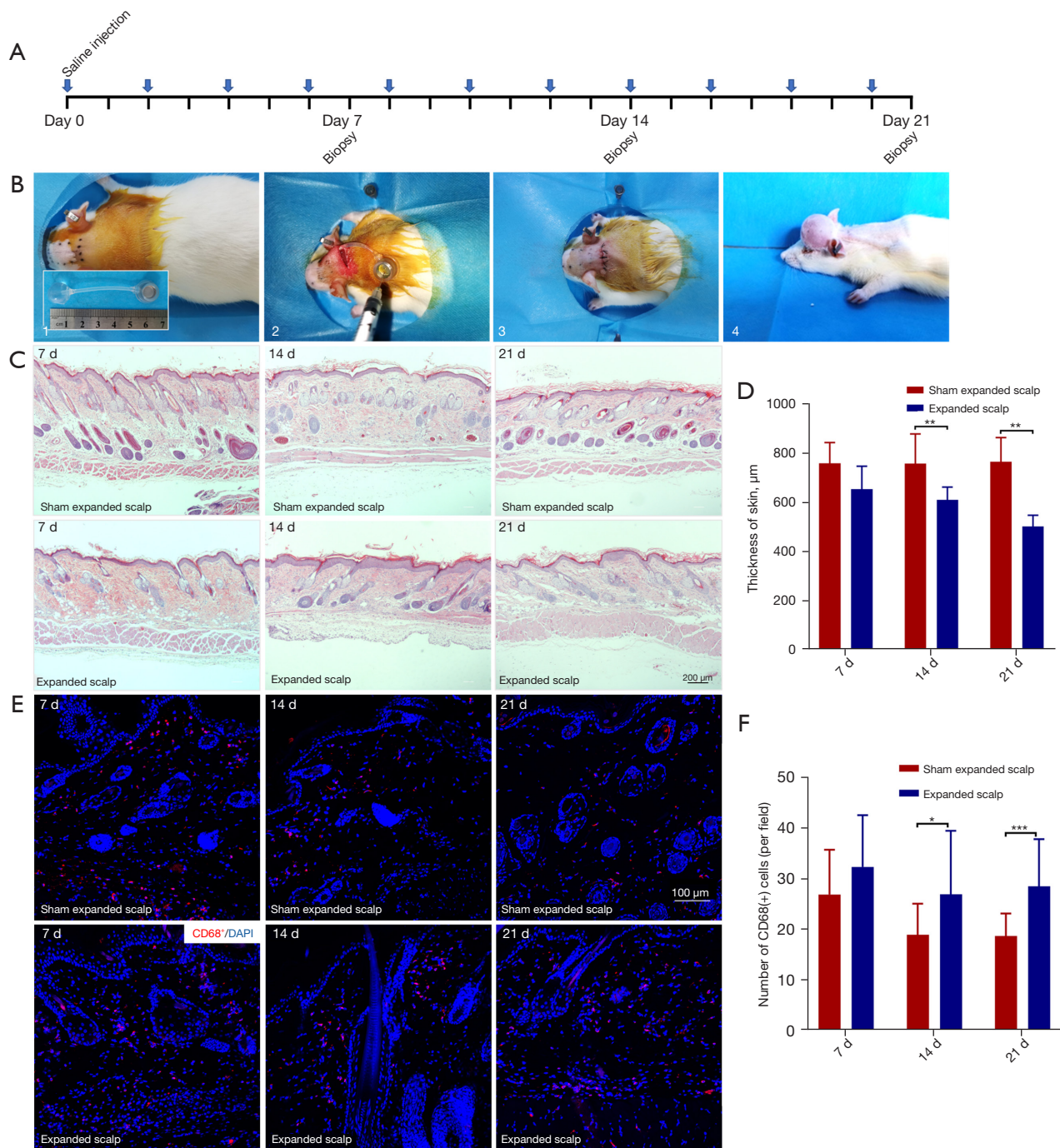


Figure 1 The number of macrophages in the scalps remained high during scalp expansion. (A) Injection schedule. Dates of saline injections for expanded scalp (\downarrow) are displayed at the top of the schedule. (B) Representative graphs of the scalp expansion model. (C) The hematoxylin and eosin staining images of rat scalp sections on days 7, 14, and 21. (D) Data from one experiment with 6 rats per time point. The thickness of the expanded scalp was thinner than the sham expanded scalp on days 14 and 21 (6 rats per time point in each group). (E) Skin sections stained with CD68⁺ (red) were used to visualize macrophages in the expanded and sham expanded scalps. (F) The total number of macrophages in the scalp was quantified. The expanded scalp had higher total macrophage levels than did the sham expanded scalp. *, $P < 0.05$; **, $P < 0.01$; ***, $P < 0.001$. DAPI, 4',6-diamidino-2-phenylindole.

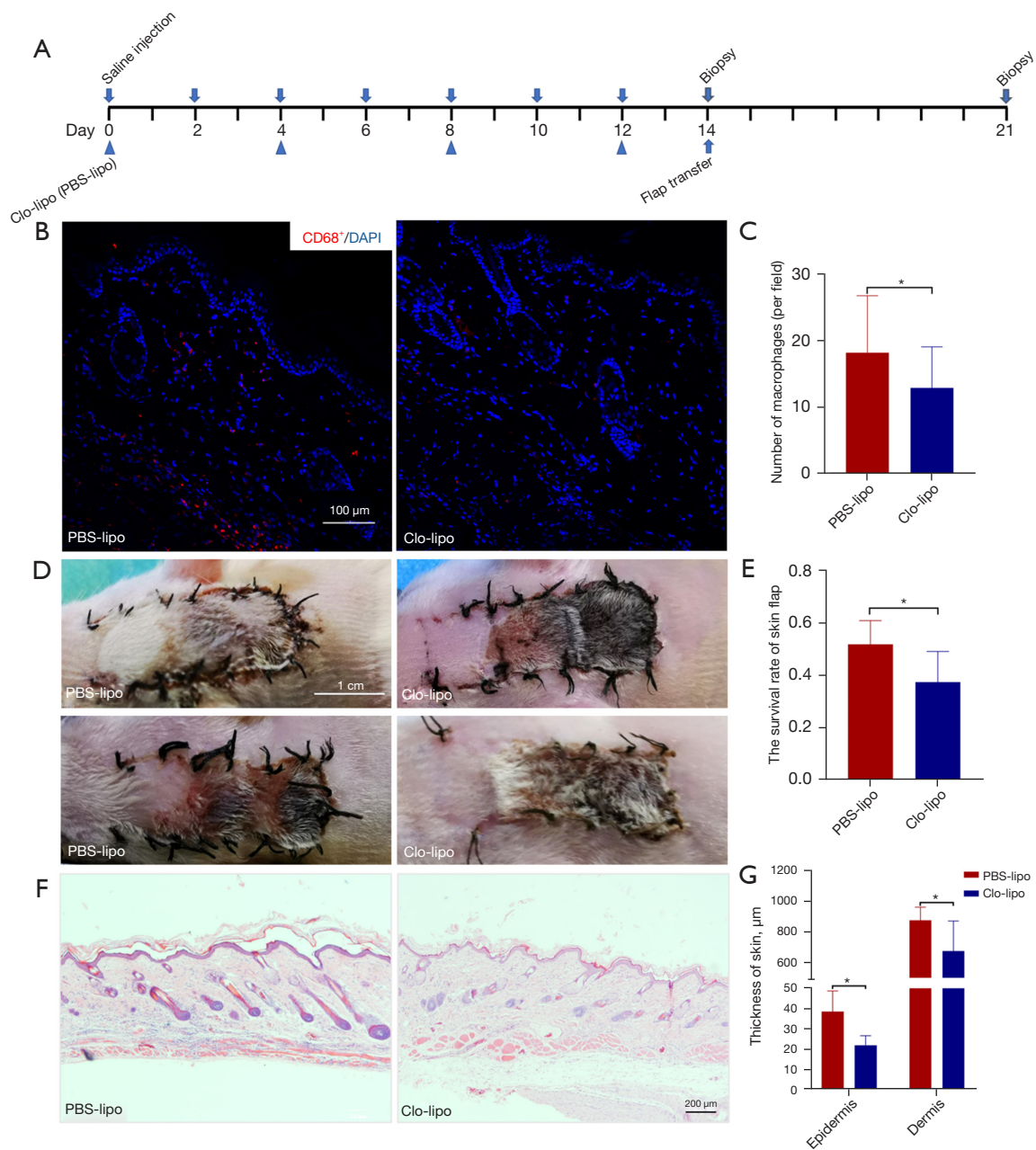


Figure 2 Macrophage depletion inhibited transferred scalp flap survival. (A) Model construction: macrophage depletion following clodronate-liposome injection during expansion and gross appearance after flap transfer. Dates of saline injections for expanding tissue and biopsy (↓) and scalp flap transfer *in situ* (↑) are displayed in the schedule. The bottom showed Clo-lipo or PBS-liposome control (PBS-lipo groups) (50 $\mu\text{g}/\text{mL}$, ▲) and time points. (B,C) Representative images of CD68⁺ macrophages (IF staining) and quantitative analysis of CD68⁺ cells. (D,E) Survived area of transferred flaps and quantitative analysis of survival rate. (F,G) Representative hematoxylin and eosin staining images of transferred expanded scalp flap and thickness analysis of the epidermis and dermis. *, $P < 0.05$. IF staining, immunofluorescence staining; DAPI, 4',6-diamidino-2-phenylindole; PBS, phosphate-buffered saline; Clo-lipo, clodronate-liposome.

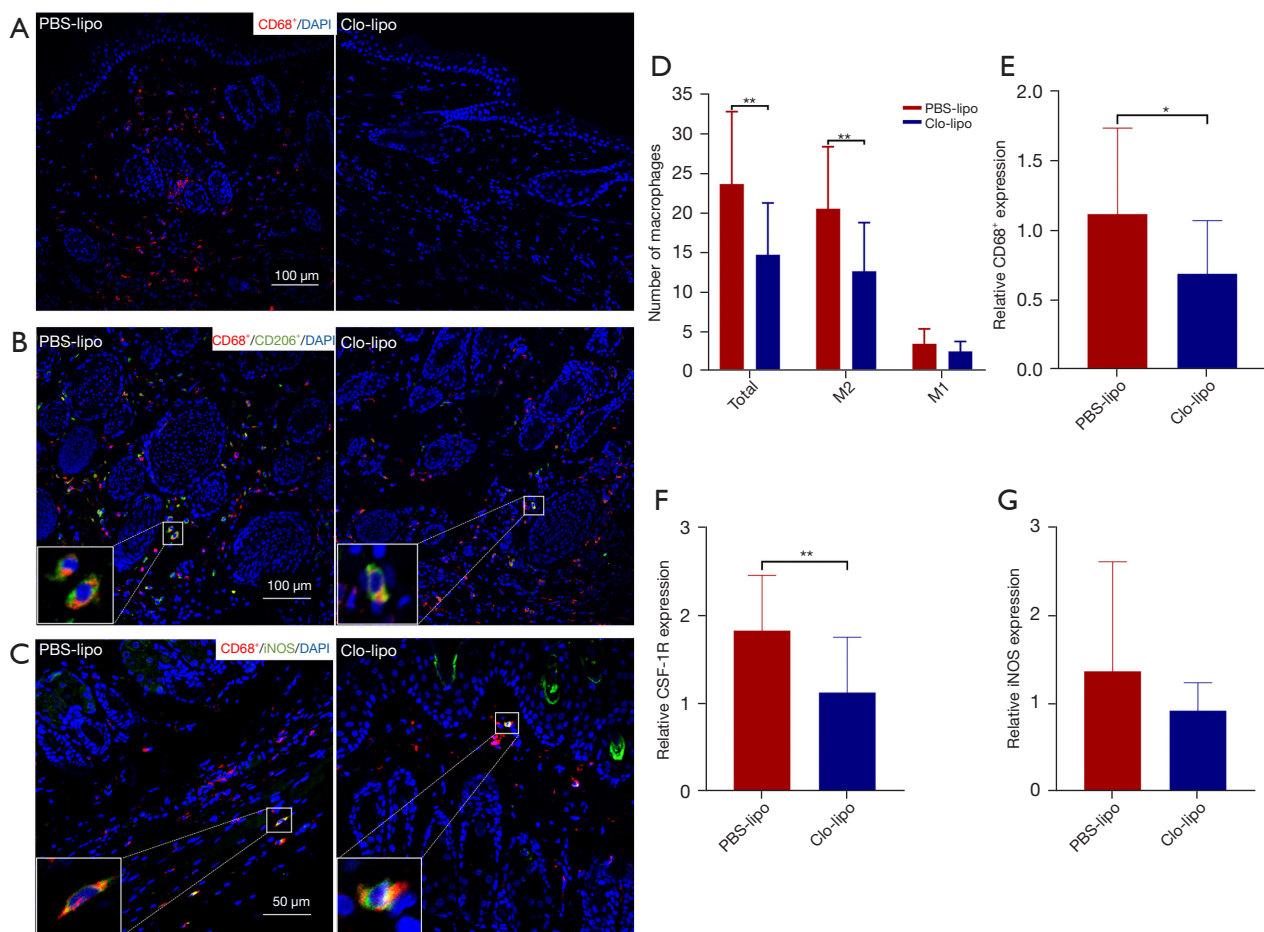


Figure 3 The changes of macrophage subtypes in the expanded scalp flap 7 days after flap transfer (day 21) by IF staining. (A) The pan-macrophage marker CD68⁺ (red) cells in the transferred flap. (B) M2 marker CD206⁺ (green) CD68⁺ (red) cells (M2 macrophages). (C) iNOS⁺ (green) CD68⁺ (red) cells (M1 macrophages). Insets show high-magnification (×40) images of the M2 or M1 macrophages. (D) The total number of macrophages (CD68⁺), M2 macrophages (CD206⁺/CD68⁺), and M1 macrophages (iNOS⁺/CD68⁺) per field. The expression of pan-macrophage marker CD68 (E) and M2 macrophage marker CSF-1R (F) dramatically decreased in the Clo-lipo group. (G) M1 macrophage marker iNOS showed no significant difference between the Clo-lipo (n=6) and PBS-lipo (n=5) groups. *, P<0.05; **, P<0.01. IF staining, immunofluorescence staining; PBS, phosphate-buffered saline; DAPI, 4',6-diamidino-2-phenylindole; Clo-lipo, clodronate-liposome; iNOS, inducible nitric oxide synthase; CSF-1R, colony stimulating factor 1 receptor.

group (Figure 5D,5E).

M-CSF treatment increased the number of macrophages in the transferred flap

The rats in the M-CSF group had significantly higher numbers of M1, M2 and total macrophages than did those in the PBS group (1-way ANOVA, total and M2: P<0.001; M1: P<0.01; Figure 6A-6D). Furthermore, M-CSF + Clo group rats had significantly fewer numbers of M1, M2, and total macrophages than M-CSF group rats (1-way ANOVA,

total and M1: P<0.001; M2: P<0.01; Figure 6A-6D). No significant difference in macrophage number was observed between the PBS and M-CSF + Clo groups (Figure 6A-6D).

Macrophages facilitate angiogenesis of the transferred flaps

The M-CSF group showed higher blood perfusion compared with that of the PBS (P<0.05), while the M-CSF + Clo group displayed relatively lower blood perfusion compared with the M-CSF group (1-way ANOVA, P<0.05; Figure 7A,7B). The M-CSF also had more CD34⁺ MVDs

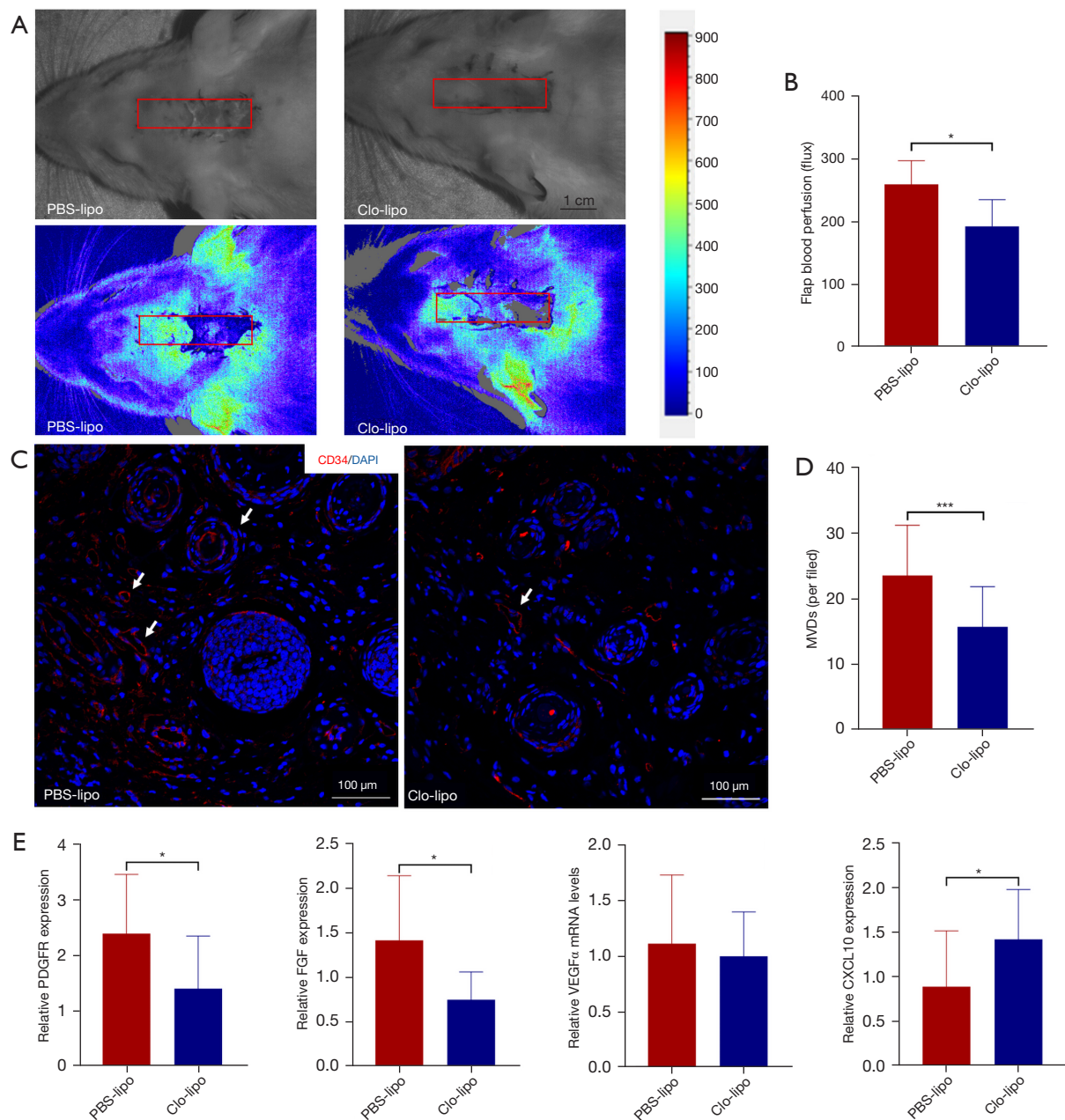


Figure 4 Macrophage depletion attenuated blood perfusion, MVDs, and the expression of angiogenic factors. (A) Representative photographs of flap blood perfusion. Red boxes indicate the transferred expanded flaps. (B) Compared with the PBS-lipo group (n=6), significantly lower blood perfusion was detected in the Clo-lipo group (n=5). (C) Representative photographs of CD34⁺ microvessels (red) in the transferred expanded scalp flap (IF staining). The white arrows indicate CD34⁺ microvessels. (D) Quantitative analysis of CD34⁺ MVDs. The number of CD34⁺ MVDs in the PBS-lipo group was higher than that in the Clo-lipo group per field. (E) Angiogenic factors, PDGFR and FGF, showed decreased expression in the Clo-lipo group versus the PBS-lipo group, while the angiostatic factor, CXCL10, showed increased expression in the Clo-lipo group versus the PBS-lipo group. No significant difference was found in VEGF α between the 2 groups. *, P<0.05; ***, P<0.001. IF staining, immunofluorescence staining; PBS, phosphate-buffered saline; Clo-lipo, clodronate-liposome; DAPI, 4',6-diamidino-2-phenylindole; MVD, microvascular density; PDGFR, platelet-derived growth factor receptor; FGF, fibroblast growth factor; VEGF α , vascular endothelial growth factor α ; CXCL10, C-X-C motif chemokine ligand 10.

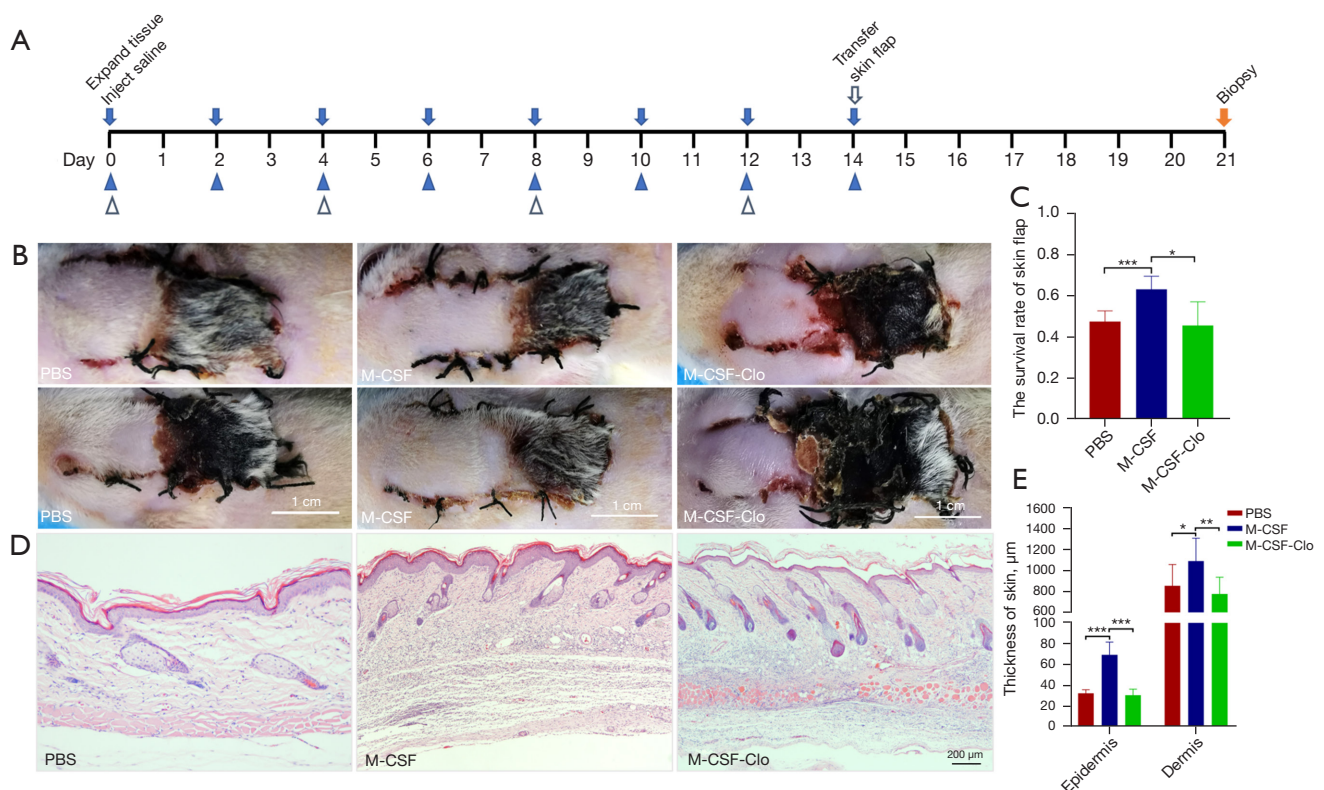


Figure 5 The survival and thickness of the expanded scalp flap after M-CSF treatment or combined M-CSF and Clo-lipo treatment. (A) Study design: dates of saline injections for expanding tissue (↓), scalp flap transfer *in situ* (⇓) and biopsy (⇓) are displayed at the top of the schedule. Dates of Clo-lipo/PBS-lipo injections (50 µg/mL, Δ) and M-CSF/PBS injections (20 ng/µL, ▲) are displayed at the bottom of schedule. (B,C) Survived area of transferred flaps and quantitative analysis of survival rate. Increased average flap survival rates were observed in the M-CSF group on day 21 (1-way ANOVA, $P < 0.001$), whereas this effect of flap survival rate (1-way ANOVA, $P < 0.05$) was reversed by M-CSF + Clo. (D,E) Representative HE staining images of transferred expanded scalp flap and thickness analysis of the epidermis and dermis. A thicker epidermis (1-way ANOVA, $P < 0.001$) and dermis (1-way ANOVA, $P < 0.05$) was observed in the M-CSF group, whereas this effect of epidermis (1-way ANOVA, $P < 0.001$) and dermis (1-way ANOVA, $P < 0.01$) was reversed by M-CSF + Clo (E). No significant difference in thickness was observed between PBS and M-CSF + Clo groups. *, $P < 0.05$; **, $P < 0.01$; ***, $P < 0.001$. PBS, phosphate-buffered saline; M-CSF, macrophage-colony stimulating factor; Clo-lipo, clodronate-liposome; HE staining, hematoxylin eosin staining; ANOVA, analysis of variance.

than did the PBS group ($P < 0.05$; Figure 7A,7B); however, this effect was reversed in the combined treatment of M-CSF and Clo-lipo groups (1-way ANOVA, $P < 0.05$; Figure 7C,7D). qRT-PCR results showed that M-CSF group had higher mRNA expression of PDGFR, FGF, and VEGF α than did the PBS group (1-way ANOVA, $P < 0.05$; Figure 7E). Compared with the Clo-lipo group, the M-CSF group showed a significant increase in the expression of PDGFR (1-way ANOVA, $P < 0.01$; Figure 7E). In addition, the M-CSF group demonstrated a lower expression of the angiostatic factor, CXCL10, compared with the control

group (1-way ANOVA, $P < 0.05$; Figure 7E) and M-CSF + Clo group (1-way ANOVA, $P < 0.05$; Figure 7E).

Discussion

Transferred skin flap is frequently used in the reconstruction of significant tissue defects (12). The survival of these skin flap presents an ongoing challenge for plastic surgeons (13), with impaired and insufficient vascularization considered commonly accepted causes of skin flap tissue necrosis (14).

Macrophages are one of the most studied cell types and

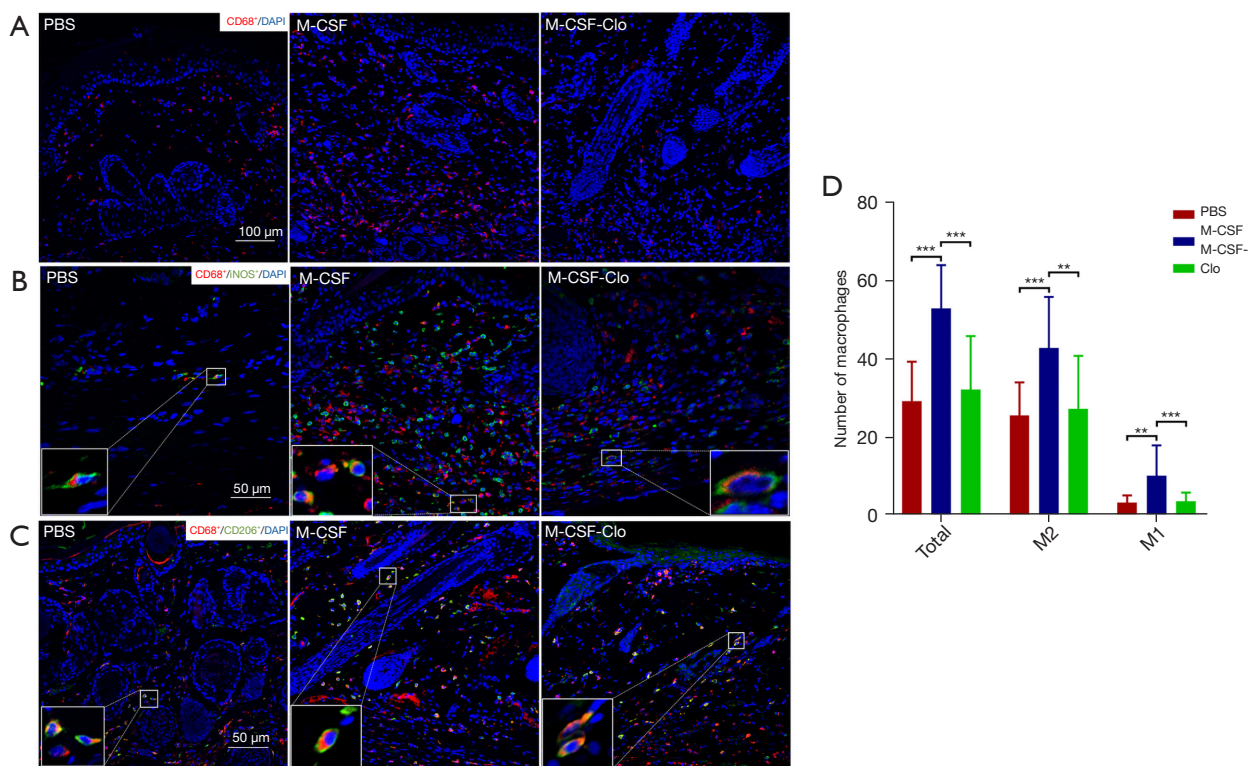


Figure 6 The number of macrophages of different subtypes in the survived flaps after transfer with PBS, M-CSF, and M-CSF + Clo-lipo treatment. (A–C) Representative IF staining images of pan-macrophages, and M2 and M1 macrophages. (A) CD68⁺ cells (red). (B) iNOS⁺ (green) CD68⁺ (red) cells (M1 macrophages). (C) Insets show high-magnification (×40) images of the M1 or M2 macrophage cells. (D) Quantitative analysis of macrophages. M-CSF group rats showed significantly higher numbers of M1, M2, and total macrophages than did the PBS group rats (1-way ANOVA, total and M2: $P < 0.001$; M1: $P < 0.01$). Furthermore, M-CSF + Clo group rats had significantly fewer numbers of M1, M2, and total macrophages than did the M-CSF group rats (1-way ANOVA, total and M1: $P < 0.001$; M2: $P < 0.01$). Total macrophages (CD68⁺), M2 macrophages (CD206⁺CD68⁺), and M1 macrophages (iNOS⁺CD68⁺). PBS group (n=6), M-CSF group (n=5) and M-CSF + Clo group (n=5). **, $P < 0.01$; ***, $P < 0.001$. PBS, phosphate-buffered saline; M-CSF, macrophage-colony stimulating factor; Clo-lipo, clodronate-liposome; ANOVA, analysis of variance; iNOS, inducible nitric oxide synthase.

are used in axolotl limb and heart regeneration (15). They promote wound healing and facilitate skin generation by promoting angiogenesis. Proangiogenic cytokines and growth factors, such as VEGF α and fibroblast growth factor 2 (FGF2), are secreted from macrophages and play an important role in angiogenesis (16,17) and macrophage activity (18,19). FGF2 is a member of FGFs family. The expression of these proangiogenic cytokines and growth factors enables macrophages to participate in the diverse phases of the angiogenic cascades, such as EC proliferation, migration, and vascular sprout formation (20–22). Expanded skin regeneration and transferred expanded flap survival in rats are dependent on angiogenesis via release of these

various proangiogenic factors derived from macrophages. Previous research has studied the role of macrophages in expanded skin regeneration (9), and this study studied this in further detail. Monocytes of other types may also contribute to expanded skin regeneration and transferred expanded flap survival in rats, which will be the focus of future study. In our rat skin expansion model, thickened expanded skin was associated with elevated macrophage levels, while macrophage depletion hindered skin regeneration during tissue expansion in the rat dorsal expansion model (9); however, to our knowledge, the effects of macrophages on angiogenesis and transferred expanded flap survival have not yet been analyzed.

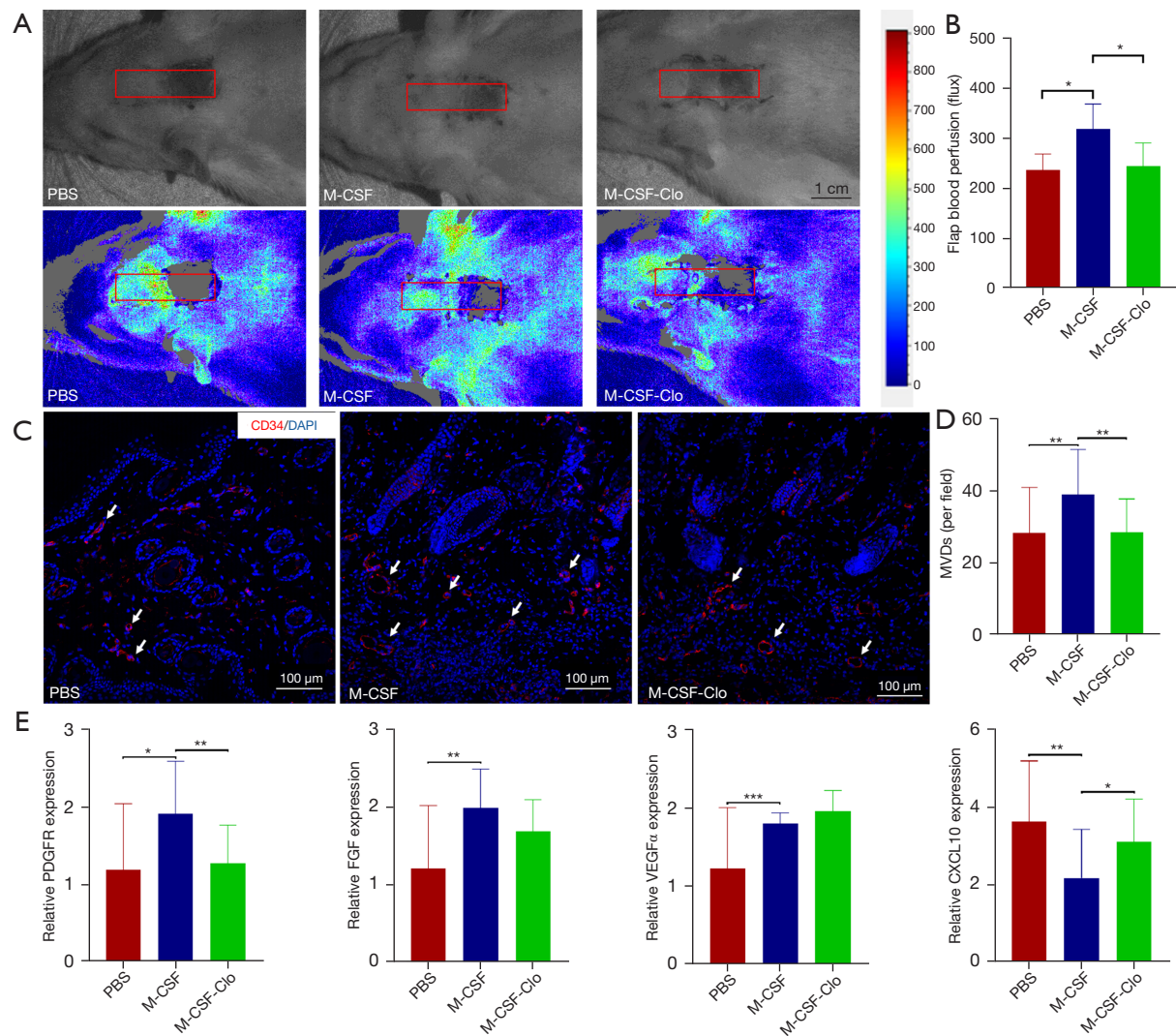


Figure 7 The effects of M-CSF treatment on the angiogenesis of scalp flap and blood perfusion, MVDs, and the expression of angiogenic factors after flap transfer. (A) Representative photographs of flap blood perfusion. Red boxes indicate the transferred expanded flaps. (B) Compared with the PBS group, significantly higher blood perfusion was observed in the M-CSF group, whereas the M-CSF + Clo group showed lower blood perfusion than did the M-CSF group. (C) Representative IF staining photographs of CD34⁺ microvessels (red) in the transferred flaps. The white arrows indicate CD34⁺ microvessels. (D) Quantitative analysis of CD34⁺ MVDs. The total number of CD34⁺ MVDs in the M-CSF group was higher than that in the PBS group, whereas M-CSF + Clo group showed a marked decrease in CD34⁺ MVDs compared with M-CSF group ($P < 0.05$). (E) Increased expression of PDGFR ($P < 0.05$), FGF ($P < 0.01$), and VEGF α ($P < 0.001$) was detected in the M-CSF group versus the control group. The M-CSF + Clo group showed lower expression of PDGFR than did the M-CSF group ($P < 0.01$). Decreased expression of CXCL10 was found in the M-CSF group versus the PBS group ($P < 0.01$), whereas CXCL10 in the M-CSF + Clo group showed a higher expression than did the M-CSF group ($P < 0.05$). PBS group, $n = 6$; M-CSF group, $n = 5$; M-CSF + Clo group, $n = 5$. *, $P < 0.05$; **, $P < 0.01$; ***, $P < 0.001$. IF staining, immunofluorescence staining; PBS, phosphate-buffered saline; M-CSF, macrophage-colony stimulating factor; Clo, clodronate; PDGFR, platelet-derived growth factor receptor; FGF, fibroblast growth factor; VEGF α , vascular endothelial growth factor α ; CXCL10, C-X-C motif chemokine ligand 10; MVD, microvascular density; ANOVA, analysis of variance.

In our preliminary study, we found that the number of macrophages on day 1 after Clo-lipo injection did not change; however, a significant change in macrophage levels was detected on day 7 (9). This and our previous study have shown that macrophage depletion during expansion impairs the survival of the transferred expanded random-pattern scalp flap through angiogenesis inhibition (9). To further investigate the effects of macrophages on angiogenesis, M-CSF was used to recruit macrophages to the expanded skin. Studies on macrophage treatments report that macrophages recruited in this fashion at the local expanded scalp guaranteed homogeneity. The results showed that local recruitment of macrophages during expansion markedly improve transferred expanded random-pattern scalp flap survival through enhanced angiogenesis.

Macrophages are the most common immune cells within the tissue microenvironment. There is growing evidence to support the role macrophages play in angiogenesis and tissue regeneration via multiple mechanisms (23). Macrophages are classified in 2 broad categories: M1 and M2 (24). In particular, M2 macrophages represent an “alternatively” activated phenotype that can promote wound healing (25). M2 macrophages have been shown to facilitate fat graft survival (26). In our previous study, we found that the M2:M1 ratio of macrophages was high in normal expanded skin, with dominance of M2 macrophages (9). In the present study, there were significantly fewer M2 macrophages following macrophage depletion and flap transfer; consequently, there was a marked reduction in flap survival after transfer, which is consistent with findings from the literature (27). Adequate blood supply plays a key role in transferred skin flap survival (28), and previous studies have demonstrated the critical role of macrophages in angiogenesis among different models (9,29,30). Moreover, M2 macrophages have been reported to play a central role in angiogenesis, tissue repair (31), regeneration of ischemic limbs (32), and the promotion of growth factor synthesis for angiogenesis (33). In this study, we also found that blood perfusion and the number of MVDs decreased after Clo-lipo treatment, along with M2 macrophages. Notably, the ability to promote angiogenesis has only been observed in M2-polarized macrophages (34). Our current research was supported that M2 macrophages contribute to angiogenesis in transferred expanded flaps.

Angiogenesis is a complex process that consists of 4 distinct steps: (I) degradation of basement membrane by protease production; (II) activation and migration of the endothelium and pericyte; (III) proliferation of ECs; and (IV)

formation of tube-like structures and capillary tubes (35).

The initial step is generation of large early angiogenic “mother vessels” from pre-existing normal venules by a process involving degradation of their rigid basement membranes (36). Following this, VEGF priming by binding VEGFR2 favors EC tubulogenesis, proliferation, and permeability. VEGF priming is also associated with the formation of actin stress fibers, activation of focal adhesion components, upregulation of the EC factor receptors, and upregulation of EC-derived PDGF, which collectively affect pericyte recruitment and proliferation (37).

In addition to modulating immune cell recruitment, macrophages also serve as angiogenesis-promoting cells by production of proangiogenic factors, such as VEGF α , FGF2, PDGFs, and matrix metalloproteinase-2 (MMP2), and by facilitating vascular reconstruction (7). A previous study suggested that angiogenic factors, such as PDGF, FGF, VEGF α , and angiostatic factor CXCL10 contributed to the survival of skin flaps (38). PDGF receptors (PDGFRs) and FGF receptors (FGFRs) are catalytic receptors with intracellular tyrosine kinase activity (39,40), and the activated forms of PDGFR and FGFR are known to play a role in angiogenesis (41). The FGF-dependent regulation of EC plays a key role in vascular growth. A decrease in hexokinase 2 levels in the absence of FGF signaling input results in decreased glycolysis, leading to impaired EC proliferation and migration (42). Part of the CD34⁺ vasa nervorum microvessels have a thick basement membrane which contains collagen fibers, and vasa nervorum endothelia and Schwann cells express FGF2 (nuclear localization) (43). VEGF α is well known for its potent angiogenic effects, which are essential for the initiation of angiogenic sprouting and for the regulation of capillary tip cell migration (44). M2 macrophages produce and relocate VEGF α to perivascular areas (45). Our study revealed that rat scalps treated with Clo-lipo showed downregulated expression of PDGFR and FGF, whereas treatment with M-CSF upregulated their expression. This observation was consistent with previous work, which found that M2 macrophages secreted PDGFB acting on PDGFR β (46), and macrophages expressed FGF1 acting on receptor FGFR1 (38). CXCL10 is a potent inhibitor of angiogenesis *in vivo* (47). It has been shown to profoundly inhibit basic FGF-induced neovascularization in athymic mice and to cause EC differentiation into tubular capillary structures *in vitro* (48). Therefore, CXCL10 contributes to the inhibition of inflammatory reaction with attracting macrophages and to angiostasis (49). Our findings showed

that CXCL10 expression was higher in the Clo-lipo group and lower in the M-CSF group. These results also supported previous work which suggested that cholesterol activation of $ERR\alpha$ may induce a transcriptional suppression of CXCL10 in macrophages (50) and that the CXCL10 gene is less expressed in M2 macrophages (51); however, treatment with both M-CSF and Clo-lipo reversed the expression pattern of PDGFs. This suggested that M2 macrophages might have contributed to angiogenesis regulation in transferred flaps by expressing PDGFR and secreting FGF, VEGF α , and CXCL10; these factors ultimately contributed to angiogenesis. Interestingly, the endogenous levels of PDGFR were downregulated in the M-CSF + Clo groups. Autocrine or paracrine loops of PDGF/PDGFR and PDGFRs may appear on the pericytes of blood vessels (39). It remains unclear why the VEGF α mRNA levels did not change in the Clo-lipo-treated expanded scalps of rats, while VEGF α expression in M-CSF-treated skin was significantly upregulated. One potential explanation is that VEGF is probably secreted from endothelial or smooth muscle cells after macrophage depletion (52), although VEGF secretion in macrophages is rapidly controlled *in vivo* (53). This speculation should be investigated in future research.

This study has a few limitations that should be addressed. For one, the specific macrophage subtypes that give rise to distinct roles in the angiogenesis and flap survival remained unexamined. However, we demonstrated that M2 macrophage depletion during expansion impaired expanded random-pattern scalp flap survival after transfer, whereas local recruitment of macrophages during expansion markedly improved expanded random-pattern scalp flap survival after transfer. Further mechanism study showed that the increased and decreased M2 macrophage levels respectively promoted and hindered angiogenesis, and that increases and decreases in angiogenesis contributed to flap blood perfusion. Therefore, the present study provides a therapeutic strategy to improve transferred expanded skin flap survival through the promotion of angiogenesis by modulating subtypes of macrophage.

Conclusions

Using rat models of scalp expansion and expanded scalp flap transfer, our study provides evidence that M2 macrophages may promote angiogenesis of expanded scalp flap and improve the survival of transferred scalp flaps. Modulating

M2 macrophages and relevant angiogenic factors may provide a key therapeutic strategy to promote expanded skin flap survival. The present results provide the basis for clinically improving random-pattern skin flap survival.

Acknowledgments

We would like to thank “Gordon L” for his help in polishing our paper.

Funding: This work was supported by the National Natural Science Foundation of China (Nos. 81971851, 82172229 and 82102347), Natural Science Basic Research Plan in Shaanxi Province of China (No. 2022JM-600), and Foundation of Xijing Hospital Grants (No. XJZT21CM33).

Footnote

Reporting Checklist: The authors have completed the ARRIVE reporting checklist. Available at <https://atm.amegroups.com/article/view/10.21037/atm-22-1558/rc>

Data Sharing Statement: Available at <https://atm.amegroups.com/article/view/10.21037/atm-22-1558/dss>

Conflicts of Interest: All authors have completed the ICMJE uniform disclosure form (available at <https://atm.amegroups.com/article/view/10.21037/atm-22-1558/coif>). The authors have no conflicts of interest to declare.

Ethical Statement: The authors are accountable for all aspects of the work in ensuring that questions related to the accuracy or integrity of any part of the work are appropriately investigated and resolved. Experiments were performed under a project license (No. IACUC-20181209) granted by the Experimental Animal Committee of the Fourth Military Medical University, and all animal surgeries were strictly performed in accordance with institutional guidelines for the care and use of animals.

Open Access Statement: This is an Open Access article distributed in accordance with the Creative Commons Attribution-NonCommercial-NoDerivs 4.0 International License (CC BY-NC-ND 4.0), which permits the non-commercial replication and distribution of the article with the strict proviso that no changes or edits are made and the original work is properly cited (including links to both the formal publication through the relevant DOI and the license).

See: <https://creativecommons.org/licenses/by-nc-nd/4.0/>.

References

1. Khouri RK, Cooley BC, Kunselman AR, et al. A prospective study of microvascular free-flap surgery and outcome. *Plast Reconstr Surg* 1998;102:711-21.
2. Zhou KL, Zhang YH, Lin DS, et al. Effects of calcitriol on random skin flap survival in rats. *Sci Rep* 2016;6:18945.
3. Wang WZ, Baynosa RC, Zamboni WA. Update on ischemia-reperfusion injury for the plastic surgeon: 2011. *Plast Reconstr Surg* 2011;128:685e-92e.
4. Kerrigan CL. Skin flap failure: pathophysiology. *Plast Reconstr Surg* 1983;72:766-77.
5. Vannella KM, Wynn TA. Mechanisms of Organ Injury and Repair by Macrophages. *Annu Rev Physiol* 2017;79:593-617.
6. Ahir BK, Engelhard HH, Lakka SS. Tumor Development and Angiogenesis in Adult Brain Tumor: Glioblastoma. *Mol Neurobiol* 2020;57:2461-78.
7. Oishi Y, Manabe I. Macrophages in inflammation, repair and regeneration. *Int Immunol* 2018;30:511-28.
8. Kim H, Wang SY, Kwak G, et al. Exosome-Guided Phenotypic Switch of M1 to M2 Macrophages for Cutaneous Wound Healing. *Adv Sci (Weinh)* 2019;6:1900513.
9. Ding J, Lei L, Liu S, et al. Macrophages are necessary for skin regeneration during tissue expansion. *J Transl Med* 2019;17:36.
10. Liu W, Xiong S, Zhang Y, et al. Transcriptome Profiling Reveals Important Transcription Factors and Biological Processes in Skin Regeneration Mediated by Mechanical Stretch. *Front Genet* 2021;12:757350.
11. Nemunaitis J, Shannon-Dorcy K, Appelbaum FR, et al. Long-term follow-up of patients with invasive fungal disease who received adjunctive therapy with recombinant human macrophage colony-stimulating factor. *Blood* 1993;82:1422-7.
12. Hanasono MM, Matros E, Disa JJ. Important aspects of head and neck reconstruction. *Plast Reconstr Surg* 2014;134:968e-80e.
13. Wei FC, Demirkan F, Chen HC, et al. The outcome of failed free flaps in head and neck and extremity reconstruction: what is next in the reconstructive ladder? *Plast Reconstr Surg* 2001;108:1154-60; discussion 1161-2.
14. Ghali S, Butler PEM, Tepper OM, et al. Vascular delay revisited. *Plast Reconstr Surg* 2007;119:1735-44.
15. Enos N, Takenaka H, Scott S, et al. Meningeal Foam Cells and Ependymal Cells in Axolotl Spinal Cord Regeneration. *Front Immunol* 2019;10:2558.
16. Xiao M, Gao L, Chandrasekaran AR, et al. Bio-functional G-molecular hydrogels for accelerated wound healing. *Mater Sci Eng C Mater Biol Appl* 2019;105:110067.
17. Xue L, Greisler HP. Angiogenic effect of fibroblast growth factor-1 and vascular endothelial growth factor and their synergism in a novel in vitro quantitative fibrin-based 3-dimensional angiogenesis system. *Surgery* 2002;132:259-67.
18. Schulze-Osthoff K, Risau W, Vollmer E, et al. In situ detection of basic fibroblast growth factor by highly specific antibodies. *Am J Pathol* 1990;137:85-92.
19. Xiong M, Elson G, Legarda D, et al. Production of vascular endothelial growth factor by murine macrophages: regulation by hypoxia, lactate, and the inducible nitric oxide synthase pathway. *Am J Pathol* 1998;153:587-98.
20. Stout RD, Jiang C, Matta B, et al. Macrophages sequentially change their functional phenotype in response to changes in microenvironmental influences. *J Immunol* 2005;175:342-9.
21. Gratchev A, Kzhyshkowska J, Köthe K, et al. Mphi1 and Mphi2 can be re-polarized by Th2 or Th1 cytokines, respectively, and respond to exogenous danger signals. *Immunobiology* 2006;211:473-86.
22. Pakala R, Watanabe T, Benedict CR. Induction of endothelial cell proliferation by angiogenic factors released by activated monocytes. *Cardiovasc Radiat Med* 2002;3:95-101.
23. Fu LQ, Du WL, Cai MH, et al. The roles of tumor-associated macrophages in tumor angiogenesis and metastasis. *Cell Immunol* 2020;353:104119.
24. Kapralov AA, Yang Q, Dar HH, et al. Redox lipid reprogramming commands susceptibility of macrophages and microglia to ferroptotic death. *Nat Chem Biol* 2020;16:278-90.
25. Han X, Huang S, Xue P, et al. LncRNA PTPRE-AS1 modulates M2 macrophage activation and inflammatory diseases by epigenetic promotion of PTPRE. *Sci Adv* 2019;5:eaax9230.
26. Cai J, Feng J, Liu K, et al. Early Macrophage Infiltration Improves Fat Graft Survival by Inducing Angiogenesis and Hematopoietic Stem Cell Recruitment. *Plast Reconstr Surg* 2018;141:376-86.

27. Jetten N, Verbruggen S, Gijbels MJ, et al. Anti-inflammatory M2, but not pro-inflammatory M1 macrophages promote angiogenesis in vivo. *Angiogenesis* 2014;17:109-18.
28. Won HR, Seo C, Lee HY, et al. An Important Role of Macrophages for Wound Margin Regeneration in a Murine Flap Model. *Tissue Eng Regen Med* 2019;16:667-74.
29. Ploeger DT, van Putten SM, Koerts JA, et al. Human macrophages primed with angiogenic factors show dynamic plasticity, irrespective of extracellular matrix components. *Immunobiology* 2012;217:299-306.
30. Lin EY, Li JF, Gnatovskiy L, et al. Macrophages regulate the angiogenic switch in a mouse model of breast cancer. *Cancer Res* 2006;66:11238-46.
31. Yotsumoto K, Sanui T, Tanaka U, et al. Amelogenin Downregulates Interferon Gamma-Induced Major Histocompatibility Complex Class II Expression Through Suppression of Euchromatin Formation in the Class II Transactivator Promoter IV Region in Macrophages. *Front Immunol* 2020;11:709.
32. Kishimoto S, Inoue KI, Sohma R, et al. Surgical Injury and Ischemia Prime the Adipose Stromal Vascular Fraction and Increase Angiogenic Capacity in a Mouse Limb Ischemia Model. *Stem Cells Int* 2020;2020:7219149.
33. White DA, Su Y, Kanellakis P, et al. Differential roles of cardiac and leukocyte derived macrophage migration inhibitory factor in inflammatory responses and cardiac remodelling post myocardial infarction. *Mol Cell Cardiol* 2014;69:32-42.
34. Schlieffsteiner C, Ibesich S, Wadsack C. Placental Hofbauer Cell Polarization Resists Inflammatory Cues In Vitro. *Int J Mol Sci* 2020;21:736.
35. Li T, Kang G, Wang T, et al. Tumor angiogenesis and anti-angiogenic gene therapy for cancer. *Oncol Lett* 2018;16:687-702.
36. Fu Y, Nagy JA, Brown LF, et al. Proteolytic cleavage of versican and involvement of ADAMTS-1 in VEGF-A/VPF-induced pathological angiogenesis. *J Histochem Cytochem* 2011;59:463-73.
37. Bowers SLK, Kemp SS, Aguera KN, et al. Defining an Upstream VEGF (Vascular Endothelial Growth Factor) Priming Signature for Downstream Factor-Induced Endothelial Cell-Pericyte Tube Network Coassembly. *Arterioscler Thromb Vasc Biol* 2020;40:2891-909.
38. Rossini M, Cheunschon B, Donnert E, et al. Immunolocalization of fibroblast growth factor-1 (FGF-1), its receptor (FGFR-1), and fibroblast-specific protein-1 (FSP-1) in inflammatory renal disease. *Kidney Int* 2005;68:2621-8.
39. Wen PY, Yung WK, Lamborn KR, et al. Phase II study of imatinib mesylate for recurrent meningiomas (North American Brain Tumor Consortium study 01-08). *Neuro Oncol* 2009;11:853-60.
40. Pan C, Nelson MS, Reyes M, et al. Functional abnormalities of heparan sulfate in mucopolysaccharidosis-I are associated with defective biologic activity of FGF-2 on human multipotent progenitor cells. *Blood* 2005;106:1956-64.
41. Gaur S, Chen L, Ann V, et al. Dovitinib synergizes with oxaliplatin in suppressing cell proliferation and inducing apoptosis in colorectal cancer cells regardless of RAS-RAF mutation status. *Mol Cancer* 2014;13:21.
42. Yu P, Wilhelm K, Dubrac A, et al. FGF-dependent metabolic control of vascular development. *Nature* 2017;545:224-8.
43. Ghinea N, Robin B, Pichon C, et al. Vasa nervorum angiogenesis in prostate cancer with perineural invasion. *Prostate* 2019;79:640-6.
44. Holderfield MT, Hughes CC. Crosstalk between vascular endothelial growth factor, notch, and transforming growth factor-beta in vascular morphogenesis. *Circ Res* 2008;102:637-52.
45. Mathivet T, Bouleti C, Van Woensel M, et al. Dynamic stroma reorganization drives blood vessel dysmorphia during glioma growth. *EMBO Mol Med* 2017;9:1629-45.
46. Li Z, Zheng M, Yu S, et al. M2 Macrophages Promote PDGFRβ(+) Pericytes Migration After Spinal Cord Injury in Mice via PDGFB/PDGFRβ Pathway. *Front Pharmacol* 2021;12:670813.
47. Struyf S, Salogni L, Burdick MD, et al. Angiostatic and chemotactic activities of the CXC chemokine CXCL4L1 (platelet factor-4 variant) are mediated by CXCR3. *Blood* 2011;117:480-8.
48. Angiolillo AL, Sgadari C, Taub DD, et al. Human interferon-inducible protein 10 is a potent inhibitor of angiogenesis in vivo. *J Exp Med* 1995;182:155-62.
49. Billottet C, Quemener C, Bikfalvi A. CXCR3, a double-edged sword in tumor progression and angiogenesis. *Biochim Biophys Acta* 2013;1836:287-95.
50. Wei W, Schwaib AG, Wang X, et al. Ligand Activation of ERRα by Cholesterol Mediates Statin and Bisphosphonate Effects. *Cell Metab* 2016;23:479-91.
51. Li C, Levin M, Kaplan DL. Bioelectric modulation of macrophage polarization. *Sci Rep* 2016;6:21044.
52. Kirito K, Fox N, Komatsu N, et al. Thrombopoietin

enhances expression of vascular endothelial growth factor (VEGF) in primitive hematopoietic cells through induction of HIF-1alpha. *Blood* 2005;105:4258-63.

53. Kottke T, Boisgerault N, Diaz RM, et al. Detecting and

targeting tumor relapse by its resistance to innate effectors at early recurrence. *Nat Med* 2013;19:1625-31.

(English Language Editors: M. Hawkins and J. Gray)

Cite this article as: Huang Z, Ding J, Song Y, Liu W, Dong C, Zhang Y, Wang T, Du J, Xiong S, He Q, Yu Z, Ma X. Macrophage contribution to the survival of transferred expanded skin flap through angiogenesis. *Ann Transl Med* 2023;11(6):248. doi: 10.21037/atm-22-1558

Table S1 PCR primer sequence

Number	Name	Sequence (5'-3')	The number of bases	Purification
01	CD68-F	TGTTCAAGCTCCAAGCCCAAA	20	PAGE
02	CD68-R	GCTCTGATGTCGGTCCTGTTT	21	PAGE
03	Csf1r-F	GCTCTGGGACCTGCTTCACTTC	22	PAGE
04	Csf1r-R	CGCTGGTCAAACAGCACATTTT	21	PAGE
05	Nos2-F	TCCTCAGGCTTGGGTCTTGTTAG	23	PAGE
06	Nos2-R	TTCAGGTCACCTTGGTAGGATTTG	24	PAGE
07	Pdgfr-F	AGTCAGTGTGAGGACTGAGCCAGA	24	PAGE
08	Pdgfr-R	TGCAAACGCGTGGTAAACAGA	21	PAGE
09	Fgf-F	GGAATTTATCAGCTTGGCTGTGG	23	PAGE
10	Fgf-R	TGTTTGACAAGGTGGATGCATAGG	25	PAGE
11	Vegfa-F	TCCTGCAGCATAGCAGATGTGA	22	PAGE
12	Vegfa-R	CCAGGATTTAAACCGGGATTTT	22	PAGE
13	Cxcl10-F	TTATTGAAAGCGGTGAGCCAAAG	23	PAGE
14	Cxcl10-R	GCTGTCCATCGGTCTCAGCA	20	PAGE
15	Rat-GAPDH-F	GGCACAGTCAAGGCTGAGAATG	22	PAGE
16	Rat-GAPDH-R	ATGGTGGTGAAGACGCCAGTA	21	PAGE